2002

Variation in the Position of the Upwelling Front on the Oregon Shelf

Jay A. Austin
Old Dominion University

John A. Barth

Original Publication Citation

Austin, J. A., & Barth, J. A. (2002). Variation in the position of the upwelling front on the Oregon shelf. *Journal of Geophysical Research: Oceans, 107*(C11), 3180. doi:10.1029/2001jc000858

Variation in the position of the upwelling front on the Oregon shelf

Jay A. Austin
Center for Coastal Physical Oceanography, Old Dominion University, Norfolk, Virginia, USA

John A. Barth
College of Oceanic and Atmospheric Sciences, Oregon State University, Corvallis, Oregon, USA

Received 5 March 2001; revised 6 March 2002; accepted 18 June 2002; published 2 November 2002.

[1] As part of an experiment to study wind-driven coastal circulation, 17 hydrographic surveys of the middle to inner shelf region off the coast of Newport, OR (44.65°N, from roughly the 90 m isobath to the 10 m isobath) were performed during Summer 1999 with a small, towed, undulating vehicle. The cross-shelf survey data were combined with data from several other surveys at the same latitude to study the relationship between upwelling intensity and wind stress field. A measure of upwelling intensity based on the position of the permanent pycnocline is developed. This measure is designed so as to be insensitive to density-modifying surface processes such as heating, cooling, buoyancy plumes, and wind mixing. It is highly correlated with an upwelling index formed by taking an exponentially weighted running mean of the alongshore wind stress. This analysis suggests that the front relaxes to a dynamic (geostrophic) equilibrium on a timescale of roughly 8 days, consistent with a similar analysis of moored hydrographic observations. This relationship allows the amount of time the pycnocline is outcropped to be estimated and could be used with historical wind records to better quantify interannual cycles in upwelling. *INDEX TERMS:* 4279 Oceanography: General: Upwelling and convergences; 4528 Oceanography: Physical: Fronts and jets; 4219 Oceanography: General: Continental shelf processes; 4223 Oceanography: General: Descriptive and regional oceanography; *KEYWORDS:* Oregon coast, upwelling, coastal circulation, relaxation, fronts

Citation: Austin, J. A., and J. A. Barth, Variation in the position of the upwelling front on the Oregon shelf, *J. Geophys. Res.*, *107*(C11), 3180, doi:10.1029/2001JC000858, 2002.

1. Introduction

[2] For physical, biological, and chemical oceanographic reasons, it is important to characterize variation in the location of the pycnocline near the coast. The outcropping of the permanent pycnocline forms an upwelling front, inshore of which nutrient-rich water from below the permanent pycnocline is exposed to the atmosphere and sunlight [*Small and Menzies*, 1981]. This leads to phytoplankton blooms, which increase the amount of energy available at the base of coastal food chains, and may promote carbon sequestration in coastal sediments. *Collins et al.* [1968] use the term "permanent pycnocline" for the strong pycnocline typically found offshore of the Oregon coast between 100 and 150 m depth. It is distinct from stronger stratification often found closer to the surface, acts as a "cap" on nutrient-rich waters below, and its hydrographic properties are largely constant over the course of a season. A naive approach to determining the frontal position might be to look at the cross-shelf distribution of surface temperature/salinity/density and locate the greatest cross-shelf gradients, or locate water with T-S properties characteristic of water typically found below the permanent pycnocline. However, there are surface processes not necessarily associated with upwelling circulation, such as heating/cooling, wind mixing, precipitation, and surface freshwater plumes, that either produce local density fronts or modify local T-S properties and may make this method unreliable. Upwelling circulation displaces isopycnals over the entire depth range and width of the shelf. By examining the displacement over the entire shelf, we can develop a robust estimate of upwelling intensity based on more information than simply the position of a given isopycnal. This estimate will be much less sensitive to non-upwelling-related variability in the hydrographic field. This measure of upwelling intensity is then compared to the alongshore wind stress, which is assumed to be the dominant force driving upwelling on this shelf.

[3] The goal of this work is twofold: to construct a robust, objective measure of the instantaneous intensity of upwelling given a cross-shelf hydrographic section, and to relate this intensity to the measured wind stress. This approach has not been pursued in the past, mainly because of a paucity of hydrographic transects at a given location over a season. Without a sufficiently large number of transects, it is difficult to obtain a relationship between the frontal position and the wind stress that has statistical significance. However, observations have provided quantitative evidence of other aspects of upwelling circulation. Moored observations have long shown saltier, cooler water on the inner shelf during upwell-

0148-0227/02/2001JC000858

ing [e.g., *Halpern*, 1976; *Winant et al.*, 1987]. Additionally, conductivity–temperature–depth (CTD) sections have shown qualitative evidence of the displacement of isopycnals due to alongshore wind stress [e.g., *Halpern*, 1974; *Huyer*, 1984]. The surface Ekman transport in several different upwelling systems was studied by *Lentz* [1992], showing quantitative agreement with the expected transport, $\frac{\tau^s}{\rho_0 f}$ [*Ekman*, 1905], where τ^s is the surface wind stress, ρ_0 the water density, and f the Coriolis parameter. Satellite images also give some sense of this displacement [*Kelly*, 1983], but they measure only the surface temperature field and therefore are sensitive to surface processes such as mixing, heating, and cooling, and can be obscured by cloud cover. Further, the permanent pycnocline tends to produce a relatively weak surface front in comparison to other surface fronts, making its location difficult to determine with only surface data.

[4] It is important to emphasize that the approach developed in this paper is not dynamical; this is simply an empirical description of pycnocline displacement and its relationship to wind forcing. Hopefully, the quantification of parameters such as a relaxation timescale will lead to future work into the dynamics that may account for such behavior. A hypothesis linking the relaxation to the alongshore pressure gradient is discussed in the last section of the paper.

[5] The number of transects collected along the Newport Hydrographic line (44.65°N) during the 1999 upwelling season allows us to make a statistically significant estimate of the relationship between the pycnocline and the wind stress. These transects include 17 made by the Oregon State University (OSU) MiniBAT group [*Austin et al.*, 2000], part of the OSU-National Oceanographic Partnership Program (NOPP) field program; six by the OSU SeaSoar group [*Barth et al.*, 2001], also part of OSU-NOPP; four by the GLOBEC Long-Term Observation Program (LTOP) [*Fleischbein et al.*, 2001]; and six as part of an OSU-NOPP biweekly sampling program (B. Peterson and L. Feinberg, personal communication, 1999), for a total of 33 transects from April to September 1999. In addition, moored data, collected as part of OSU-NOPP, are available and are used to verify the relaxation scales estimated using the transect data.

[6] Since this is the first paper to contain results from the OSU-NOPP MiniBAT program, a short description of instrumentation and cruise procedure is provided in section 2. Section 3 presents a short sampling of the MiniBAT observations. Section 4 will provide an analysis of the position of the permanent pycnocline using the data from the programs listed above. This is followed by a discussion of some implications of this research, and some concluding remarks (section 5).

2. The MiniBAT Field Program

[7] The MiniBAT (Guildline Instruments) is a small, towed, undulating vehicle which operates on the same principle as a SeaSoar [*Pollard*, 1986]. The main advantage of the MiniBAT is its small size, which allows it to be deployed from a small vessel, in shallow water, with only two scientific crew. This keeps costs down and increases scheduling flexibility. The vehicle used in this study carried a Sea-Bird Electronics SBE-25 CTD with pumped T/C sensors, a Western Environmental Technology Laboratories (WETLabs) WetStar single-channel fluorometer and C-star transmissometer. All of these instruments sampled at 8 Hz. The vehicle is towed behind a boat, in our case the 37 foot R/V *Sacajawea*, using a 200 m, 3/8″ (0.95 cm), hair-faired seven-conductor cable and a portable battery-powered winch. Full towing speed was typically 6 knots (3.1 m s^{-1}). The wing position, which determines whether the vehicle climbs or dives, is controlled from a deck unit. The original wings supplied by the manufacturer were replaced with larger, more hydrodynamic wings for the 29 June cruise and all subsequent cruises. All of the CTD data, as well as engineering data (depth and measured wing angle) are transmitted to a pair of laptop computers and stored. The ship was instrumented with a GPS and depth sounder to determine position and local water depth. A typical cross-shelf section (Figure 1) is obtained by towing the MiniBAT from roughly the 90 m isobath (29 km offshore) shoreward to roughly the 8 m isobath, depending on the sea state. Cross-shelf surveys took approximately 6 hours of ship time, 2.5 hours of which was actual sampling time. Surveying was limited only by wave state, and more specifically, by the presence of wind waves. Wind waves of more than approximately 2 m made work too difficult and dangerous to complete. This will inherently introduce some bias to the measurements, as we were unlikely to sample in strong winds. Waves off the central Oregon coast greater than 2 m occurred about 20% of the time between June and September.

[8] The vertical sampling range of the vehicle is a function of its instrument payload and trim, towing speed, and wing area. At full ship speed the vehicle could typically be maneuvered between the surface and approximately 60 m depth. To obtain data closer to the bottom, the ship was placed in idle when the vehicle reached the bottom of its descent. This allowed the vehicle to sink under its own weight. Once the vehicle had come close to the bottom (frequently within 3 m), the ship was brought back to full speed, and it would profile to the surface. No significant difference in data quality was observed between the upcast and the downcast and both are used in the following analysis. Each full cycle of the vehicle took approximately 1 km of horizontal travel when in deep water, and considerably less in shallow water. The vehicle could profile to the surface, but was typically turned around at approximately 0.5–1 m in order to keep the vehicle out of the surface waves. Depending on the sea state, the survey would either be halted at approximately the 18 m isobath, just offshore of a large submarine reef where larger waves frequently break, or would be continued inshore of the reef into water as shallow as 8 m.

[9] Once the data were collected, it was postprocessed to remove any clear outliers, and the data from the GPS and depth sounder were synchronized with the CTD data. The data were then interpolated onto a grid using a Gaussian decorrelation function with a horizontal length scale of 2.5 km (for details of the MiniBAT data acquisition and processing, see the work of *Austin et al.* [2000]). Although a large amount of short timescale hydrographic variation was observed at the OSU-NOPP moorings (Figure 2) placed along the NH line [*Boyd et al.*, 2000], much of this variation is smoothed over in the gridding process. The temperature and salinity fields are used to derive σ_t. The transmissivity, which is measured as the fraction of light which traverses

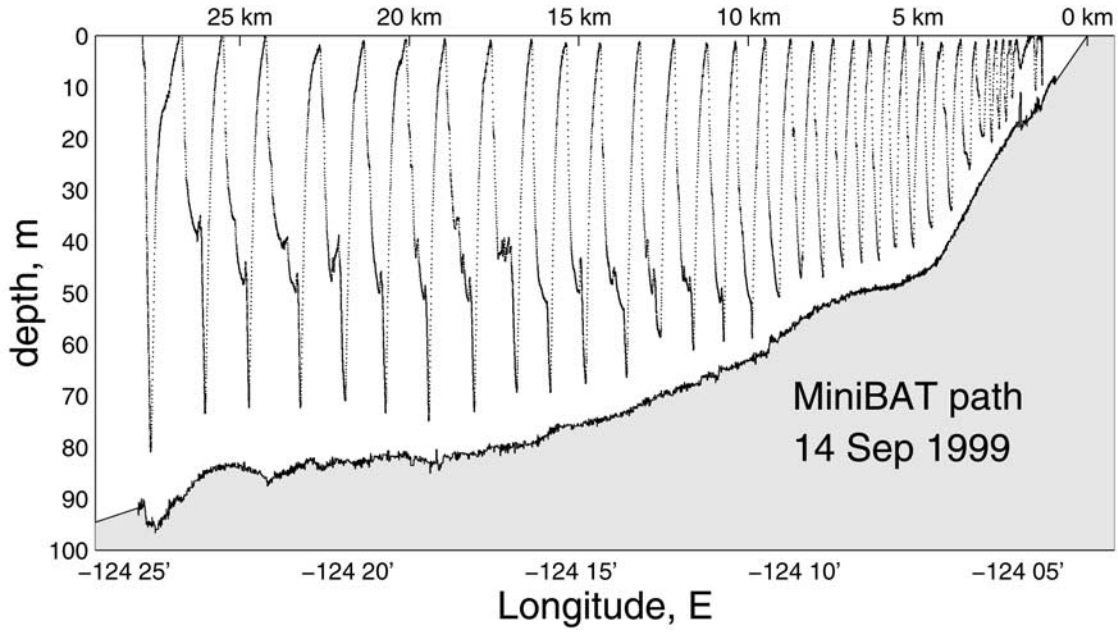

Figure 1. The vehicle path from the 14 September cruise, demonstrating the high horizontal resolution achieved by the MiniBAT.

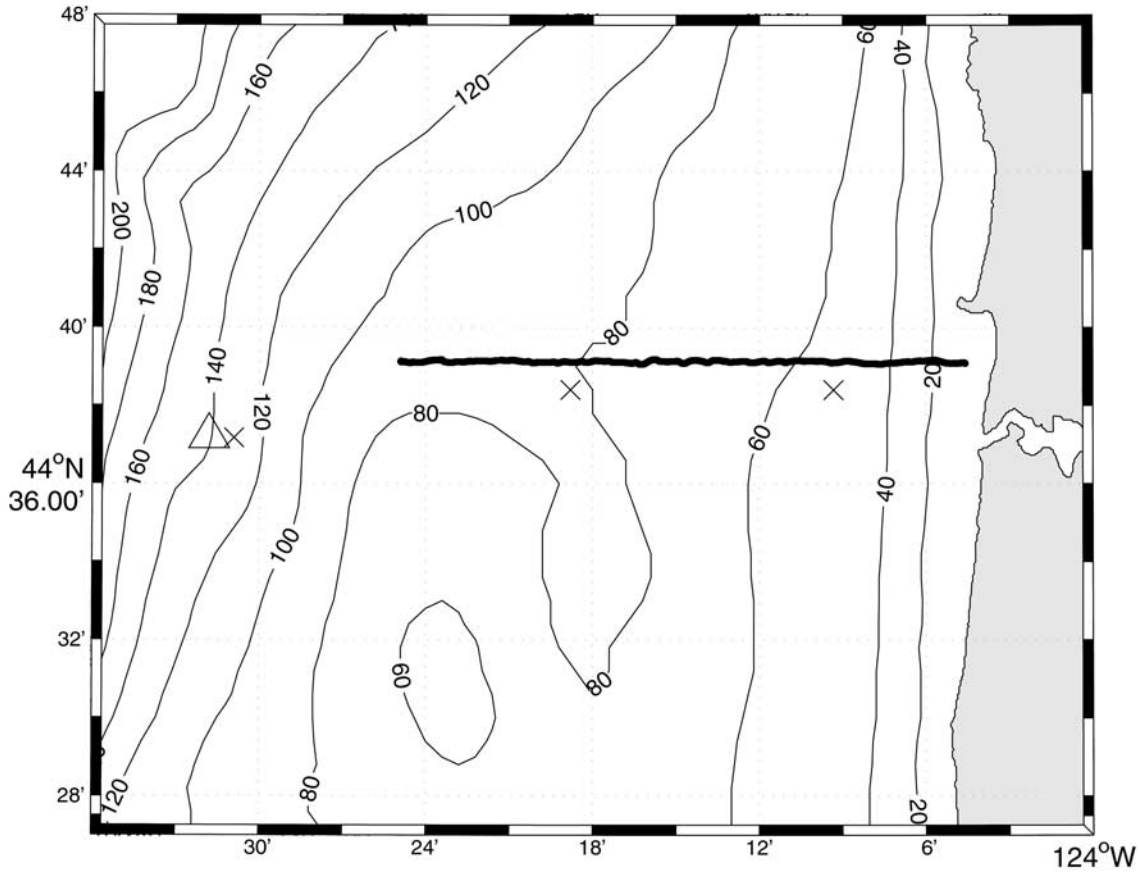

Figure 2. A plan view of the MiniBAT cruise track used, with the 50, 80, and 130 m moorings of *Boyd et al.* [2000] marked with x's. NDBC 46050 is marked with a triangle. Bottom contours are in meters.

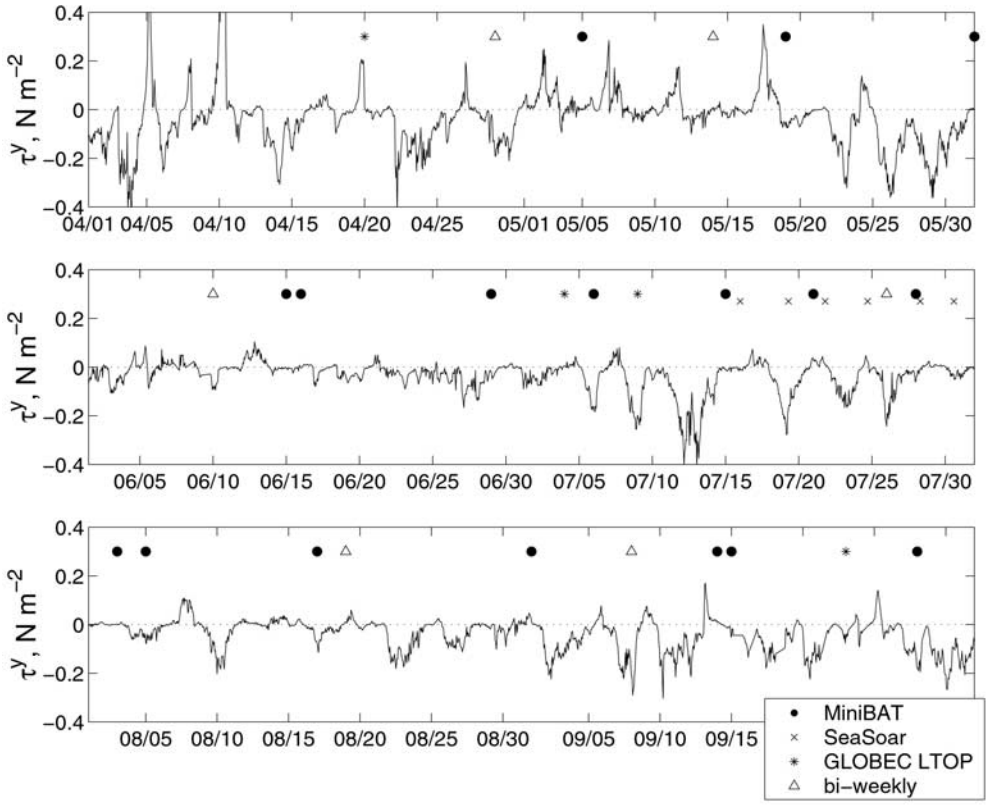

Figure 3. Cruises along the Newport Hydrographic line (44.65°N) during 1999. These include 17 cruises by the MiniBAT, six by the OSU SeaSoar group, four by the GLOBEC LTOP program, and six NOPP biweekly cruises. The alongshore wind stress is shown, taken from NDBC buoy 46050, roughly 37 km offshore.

the instrument's 25 cm beam path, is converted to an *e*-folding length scale, and are presented in meters. The fluorometer voltage is left unprocessed, since the conversion between the voltage and chlorophyll content can be partially dependent on species composition, which was unknown, but in general higher voltages correspond to higher chlorophyll concentrations.

3. Data

[10] The MiniBAT field season consisted of 17 transects of the Newport Hydrographic line (44.65°N) (the focus of this paper), two radiator surveys which consisted of smaller cross-shelf surveys at three different latitudes, and an alongshore survey roughly along the 30 m isobath. The cross-shelf surveys took place between 5 May 1999 and 28 September 1999 (Figures 2 and 3). The surveys are shown here along with the alongshore wind stress, derived using the TOGA-COARE algorithm for wind stress [*Fairall et al.*, 1996], and wind speed measured at NDBC buoy 46050, roughly 37 km offshore. Surveys before 1 June did not have the good vertical coverage of those thereafter as we were still developing our sampling techniques. There does not appear to be any significant evolution of the basic hydrographic properties over the season between the beginning of June and the end of September: all of the surveys show approximately the same range in temperature, salinity, and stratification, as well as the turbidity and fluorescence fields. The hydrographic variation between sections appears to be mainly related to the intensity of upwelling winds (to be discussed in section 4) and occasional freshwater intrusions from the Columbia River 160 km to the north.

[11] The frequency of the surveys increased from one every few weeks up to two per week during the latter half of July, when the R/V *Wecoma* was doing SeaSoar towed surveys of a larger area offshore of Newport [*Barth et al.*, 2001]. The surveys on 20 and 27 July were "box" surveys, and the 18 August survey was an alongshore survey from 44.83°N to 44.33°N, approximately along the 30 m isobath. Some of these surveys took place on successive days, and these pairs will eventually be used to study variation in the hydrographic field on short timescales. Likewise, the box surveys and the alongshore surveys will be used to study alongshore variation. In this section we discuss data from two MiniBAT surveys: 15 July, immediately after a strong upwelling event, and 1 September, taken during a period of relative calm. A complete presentation of all of the 1999 MiniBAT surveys can be found in the work of *Austin et al.* [2000].

[12] As a great deal of historical data from this region are available in the literature [e.g., *Huyer et al.*, 1975; *Halpern*, 1976], we will not dwell on the gross features of the hydrography as their basic characteristics are consistent with historical data. Namely, isopycnals slope upward toward the coast, changes in density are dominated by salinity throughout most of the water column, and temper-

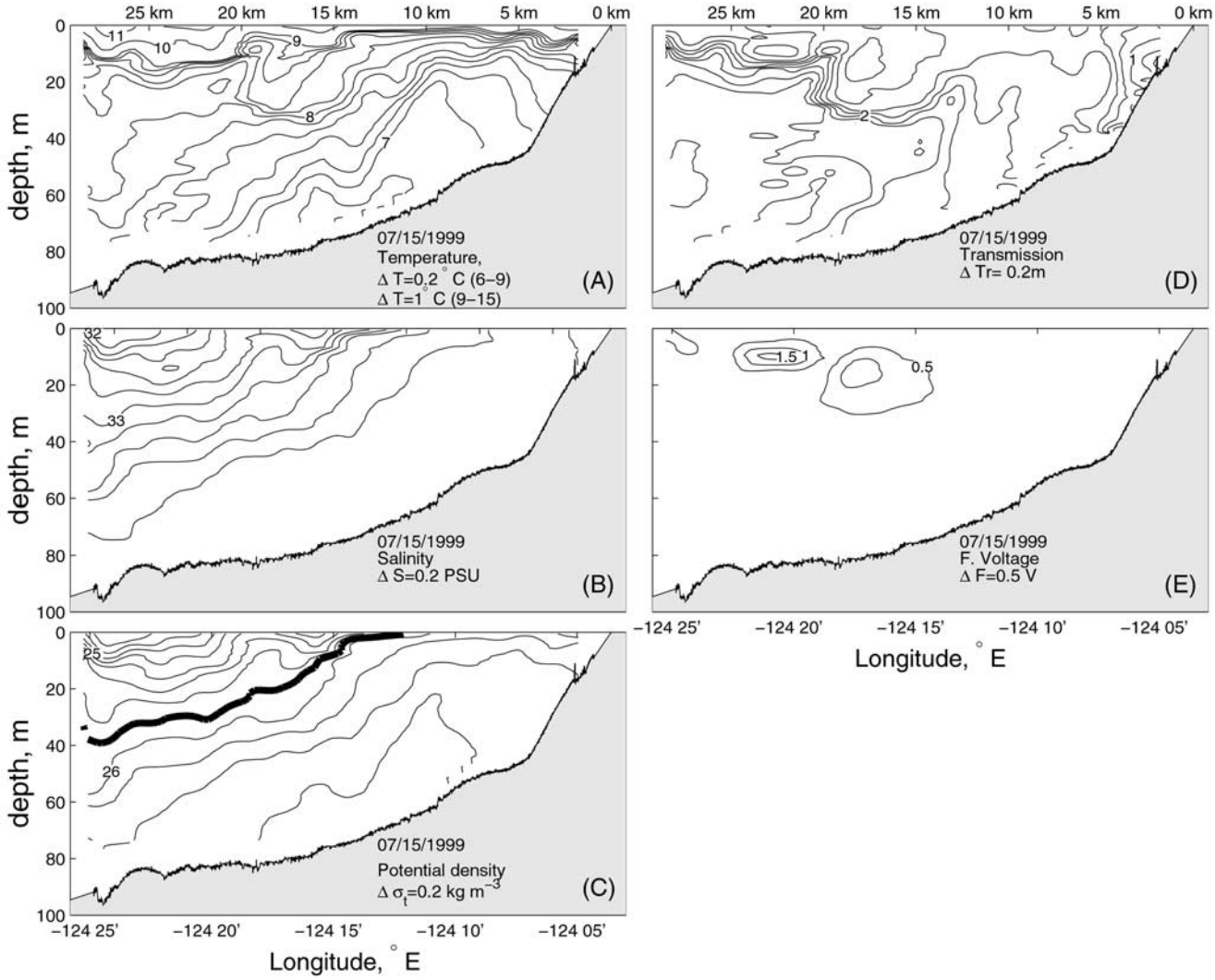

Figure 4. Data from the 15 July 1999 cruise taken along 44.65°N (Figure 2, NH line). (A) Temperature. (B) Salinity. (C) Potential density. Heavy line is the 25.8 σ_t isopycnal. (D) Transmissivity. (E) Fluorometer voltage.

ature plays a role in determining density near the surface. Light transmission near the surface and near the coast is low, and chlorophyll concentration is high near the coast. However, due to the scarcity of high horizontal resolution observations in shallow coastal waters, we present two sections that are representative of strong upwelling conditions (15 July) and relatively weak upwelling conditions (1 September).

3.1. 15 July 1999 Survey

[13] The survey taken on 15 July represents one of the most strongly upwelled sections of the field season (Figure 4). It was taken following a large upwelling-favorable wind event which lasted for approximately 3 days, from 11 to 14 July, with peak stresses on the order of 0.4 N m^{-2}. This survey contains the lowest temperatures recorded during any of the MiniBAT transects (<6.8°C), and shows the 25.8 σ_t isopycnal (which is a good proxy for the upwelling front, as will be shown) displaced approximately 15 km offshore at the surface. The fluorometer voltage and the turbidity are both low, suggesting that the region has recently been ''flushed'' with phytoplankton-poor water, and a bloom has not had time to form since the (presumably nutrient rich) water reached the surface [*Small and Menzies*, 1981].

3.2. 1 September 1999 Survey

[14] Another cross-shelf survey on 1 September (Figure 5) was taken after several weeks of relatively weak alongshore winds. The isopycnals are clearly deflected up toward the coast suggesting that the ''relaxed'' state of the shelf is still characterized by a strong upwelling signal, presumably balanced by the persistent alongshore jet. In addition, this section showed evidence of temperature inversions similar to those observed in previous studies [*Pak et al.*, 1970; *Huyer and Smith*, 1974]. The warm water intrusion appears to originate about 10 km offshore and extends out of the study region. SeaSoar surveys done in the same area earlier in the season show this inversion layer extending across the shelf at least 60 km offshore. This ''tongue'' is reflected in the turbidity and the fluorometry signals as well, further

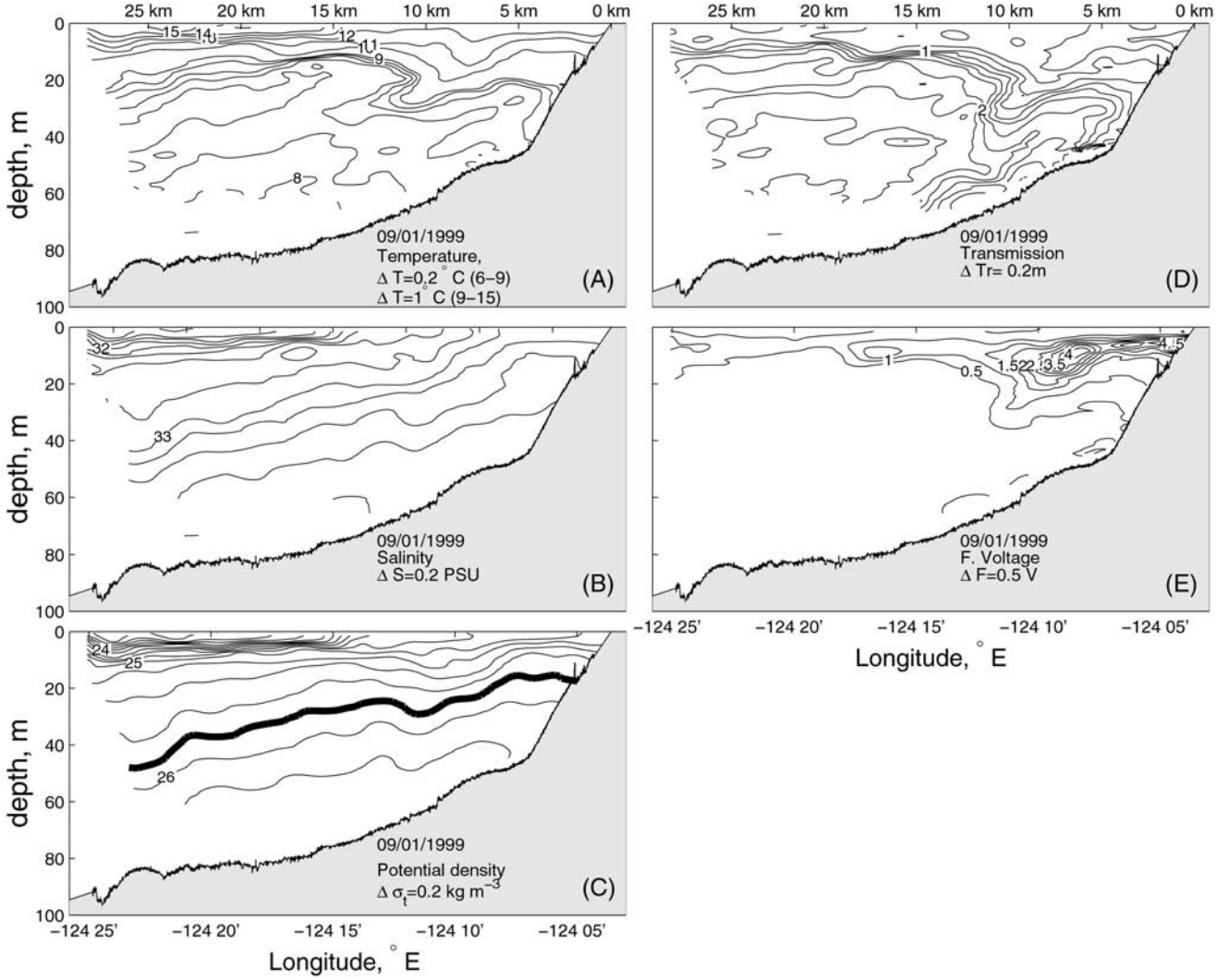

Figure 5. Data from the 1 September 1999 cruise taken along 44.65°N (Figure 2, NH line). (A) Temperature. (B) Salinity. (C) Potential density. Heavy line is the 25.8 σ_t isopycnal. (D) Transmissivity. (E) Fluorometer voltage.

suggesting that this is an intrusion process. *Pak et al.* [1970] suggest that this structure is due to upwelled water becoming heated at the coastal boundary and being subducted as it is moved offshore.

4. Analysis of Frontal Position

4.1. The Main Pycnocline

[15] There is a permanent (nonseasonal) pycnocline at an offshore depth of approximately 125 m during the spring of 1999 (Figure 6A). Evidence from other LTOP cruises (Figures 6A and 6B), a SeaSoar section (Figure 6C) as well as historical data [*Collins et al.*, 1968; *Mooers et al.*, 1976] suggest that this is a consistent feature off the Oregon coast. Moreover, both recent surveys and historical data suggest that this pycnocline is often characterized by water of densities between 25.5 and 26 kg m^{-3}, and nutrient concentrations tend to be heightened below this level. Since the stratification in this pycnocline can be relatively weak near the coast, we first justify the use of the 25.8 σ_t surface as a proxy for the main pycnocline.

[16] As the season progresses into summer, the strength of this pycnocline is swamped by surface stratification brought upon by heating and freshwater inputs. However, sections taken by the SeaSoar in July 1999 suggest that the pycnocline around 25.8 σ_t persists, having the strongest stratification outside the surface stratification. In addition, sections from along the coast [e.g., *Barth et al.*, 2001] show that this depth and density of the deep N^2 maximum are roughly constant within 100 km north or south of the NH line.

[17] Nutrient data (Figure 7) were taken during the GLOBEC LTOP hydrographic cruise in July 1999. An example of this data (other nutrients showed a similar distribution) shows that the 25.8 σ_t (shown as a heavy dashed line) is also roughly coincident with the nitrocline. This suggests that the outcropping of the main pycnocline will likely result in increased photosynthetic activity, as the nutrient-rich deeper waters are brought into the euphotic zone. The extinction depths for light, especially near the coast, are very shallow, and it is assumed for the sake of argument that the surface outcropping will serve as an

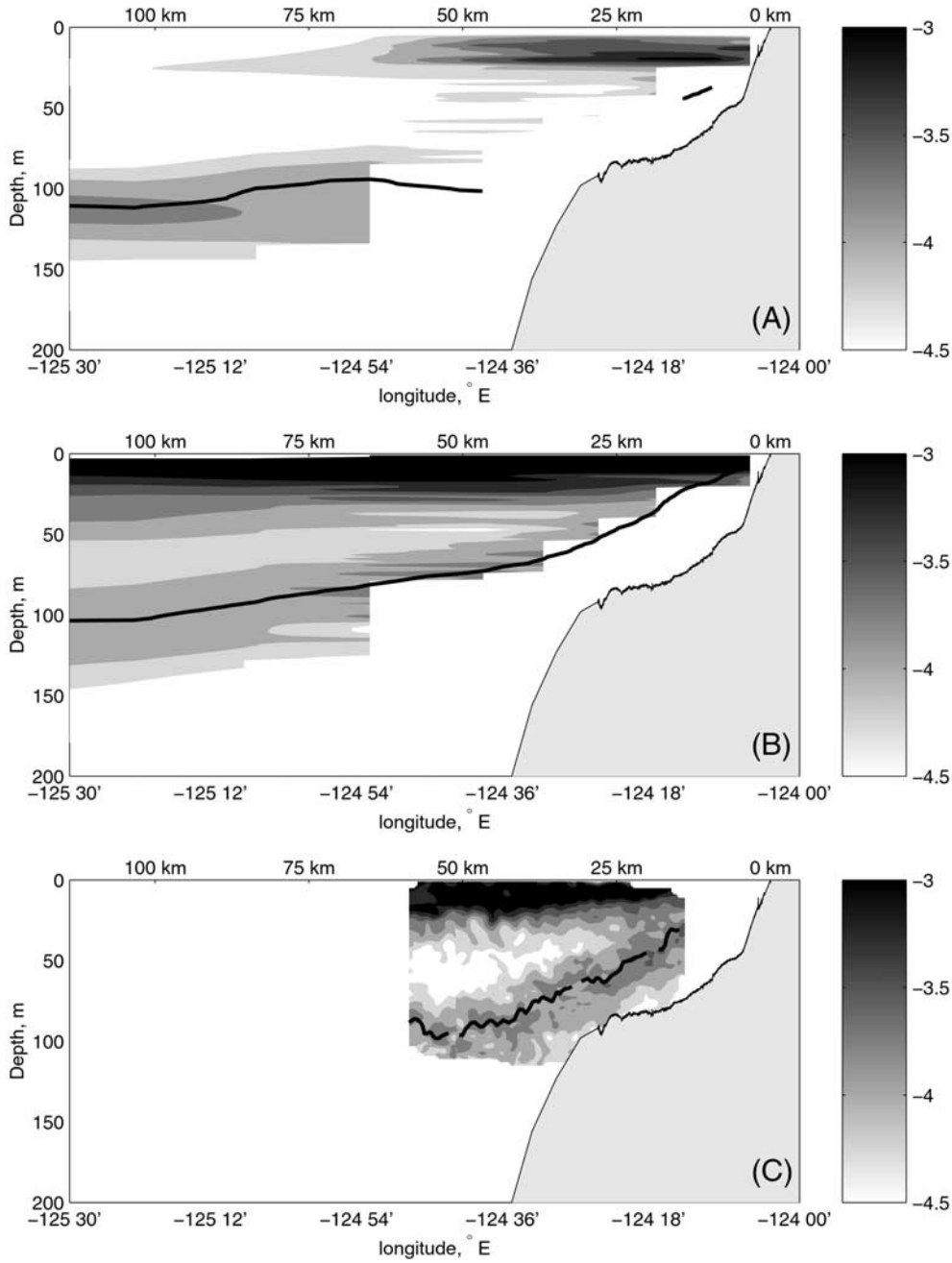

Figure 6. The log of the buoyancy frequency squared, showing the permanent pycnocline, with the 25.8 σ_t isopycnal superimposed. (A) GLOBEC-LTOP, w9904b (20 April 1999). (B) GLOBEC-LTOP, w9907a (4 July 1999). (C) OSU-NOPP SeaSoar Big-Box 1 (15 July 1999). GLOBEC-LTOP data courtesy of Jane Huyer and Robert Smith, OSU.

effective indicator of whether light is reaching nutrient-rich water.

4.2. Quantifying the Position of the Pycnocline

[18] In order to quantify the relationship between pycnocline displacement and the alongshore wind stress, some objective measure of the pycnocline position must be established. We have shown so far that there is a subsurface N^2 maximum in the spring–summer, and that it tends to be coincident with a particular σ_t level. The location of the 25.8 σ_t isopycnal at the surface could be used; however, many processes besides advection due to upwelling influence the density structure near the surface. Additionally, basing the estimate of the position of the front on a single measurement is not robust, as the estimate would be contaminated by short timescale variation inherent in the hydrographic field. Most of the CTD data collected come in the form of cross-shelf surveys, showing the variation of the depth of isopycnals across the shelf. By fitting an appropriate curve to all of the available data on the isopycnal of interest, a more robust estimate of the frontal position is attained. In addition, this method allows the upwelling intensity to be

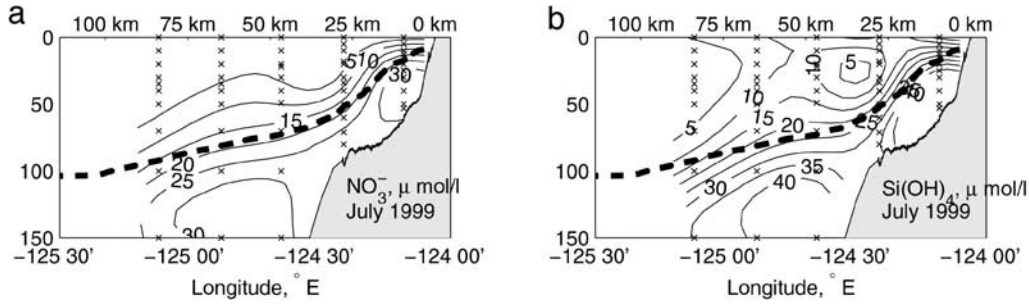

Figure 7. Distribution of (a) nitrate and (b) silicate during the July 1999 GLOBEC-LTOP hydrographic cruise. The small x's represent the location of the nutrient sampling. The heavy dashed line is the 25.8 σ_t. Nutrient data courtesy of Pat Wheeler and Holly Corwith, OSU.

estimated even if the coverage of the shelf by a survey is incomplete. The natural choice for a model to fit the 25.8 σ_t isopycnal is an exponential curve, as the Rossby adjustment problem suggests this as the natural equilibrium shape of an isopycnal in a two-layered fluid [*Gill*, 1982, pp. 191–194]. In addition, *Mooers et al.* [1976] show that isopycnals on the Oregon shelf have approximately an exponential profile, though they also suggest that the horizontal length scale is larger on the continental slope (O(68 km)) than it is on the shelf (O(42 km)). The following analysis will assume a single radius of deformation for a given hydrographic section, regardless of cross-shelf position. Therefore, the following model will be used:

$$h(x) = -H + Ae^{x/R}, \tag{1}$$

where H is the offshore depth of the 25.8 σ_t, taken to be 125 m, $h(x)$ is the idealized depth of the 25.8 σ_t, z is the

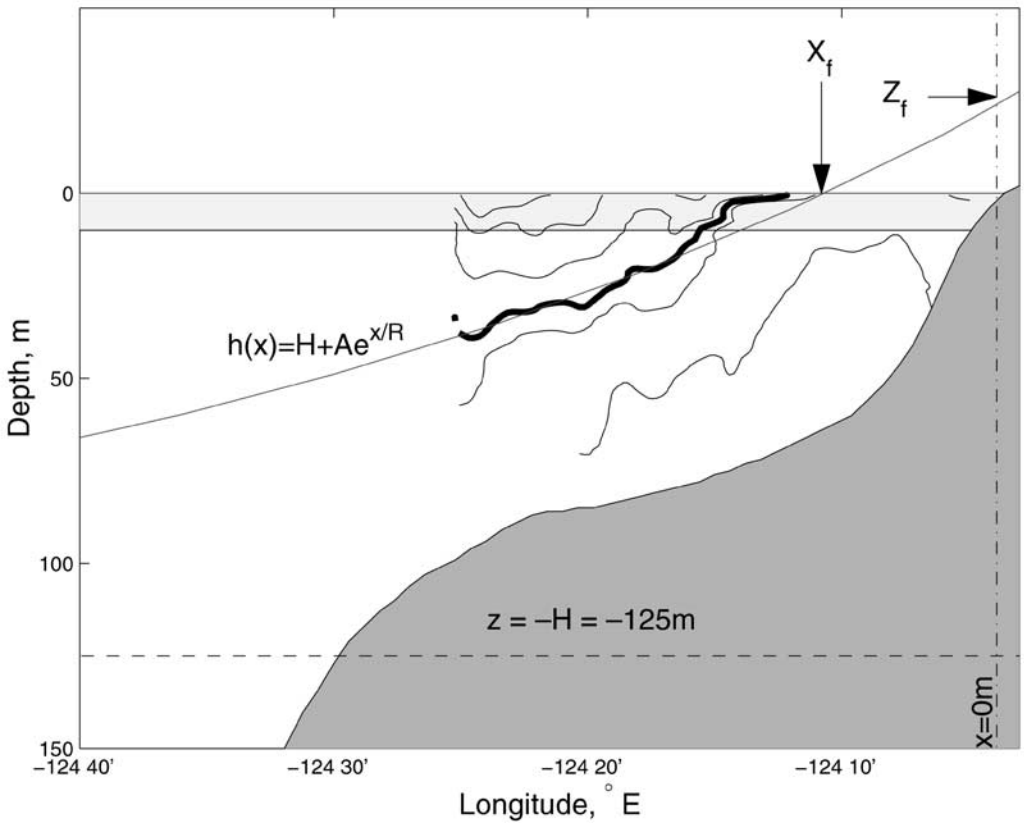

Figure 8. Schematic description of terms used in the pycnocline analysis: the coordinate system, where $x = 0$ is the coast, $z = 0$ the water surface, H is the offshore depth of the pycnocline, here 125 m, X_f is the extrapolated position of the upwelling front, and Z_f is the vertical position of the upwelling front at the coast. The heavy line is the 25.8 σ_t; the light line is the best fit of equation (1) to it. The light gray area at the surface is the top 10 m, which is ignored in making the fit. The data are the density field from the 15 July MiniBAT cruise.

Table 1. Relative Coverage of the Four Observational Programs Along the NH Line

Program	Spatial Extent, km	Casts/ Transect	Transects (-Discarded Transects)
OSU-NOPP MiniBAT	~30	~60	17-2
OSU-NOPP SeaSoar	~60	~100	6
GLOBEC-LTOP	~200	12	4-1
NOPP biweekly	~30	5	6

height (defined as $z = 0$ at the surface and positive upward), x is the cross-shelf position (defined as $x = 0$ at the coastline and positive eastward), and A and R are to be determined. The rest of the analysis is not particularly sensitive to the value used for σ_t. The value of H was estimated using data from the 1999 LTOP surveys, which extended considerably further offshore and deeper than the MiniBAT surveys. LTOP data from several seasons suggest H stays reasonably constant over an upwelling season. This allowed us to use $H = 125$ m as the far offshore pycnocline depth even in surveys that never reached this depth, such as the MiniBAT surveys.

[19] In order to estimate the best fit parameters for A and R given a cross-shelf section, a numerical minimization routine is used to make a least squares estimate of the optimal values of A and R. Since the fit is nonlinear, error estimates are made using a Monte Carlo-type method. In these fits, data taken from shallower than 10 m are assumed to be influenced by surface processes such as mixing, heating/cooling, and buoyancy sources, and is not used. Near the surface, the main pycnocline is obscured by the strong local stratification, and the 25.8 σ_t may not be representative of the main pycnocline near the surface. The error in the determination of the depth of the 25.8 σ_t level is estimated using the mooring data [*Boyd et al.*, 2000]. It appears that the variance in the depth of the 25.8 σ_t

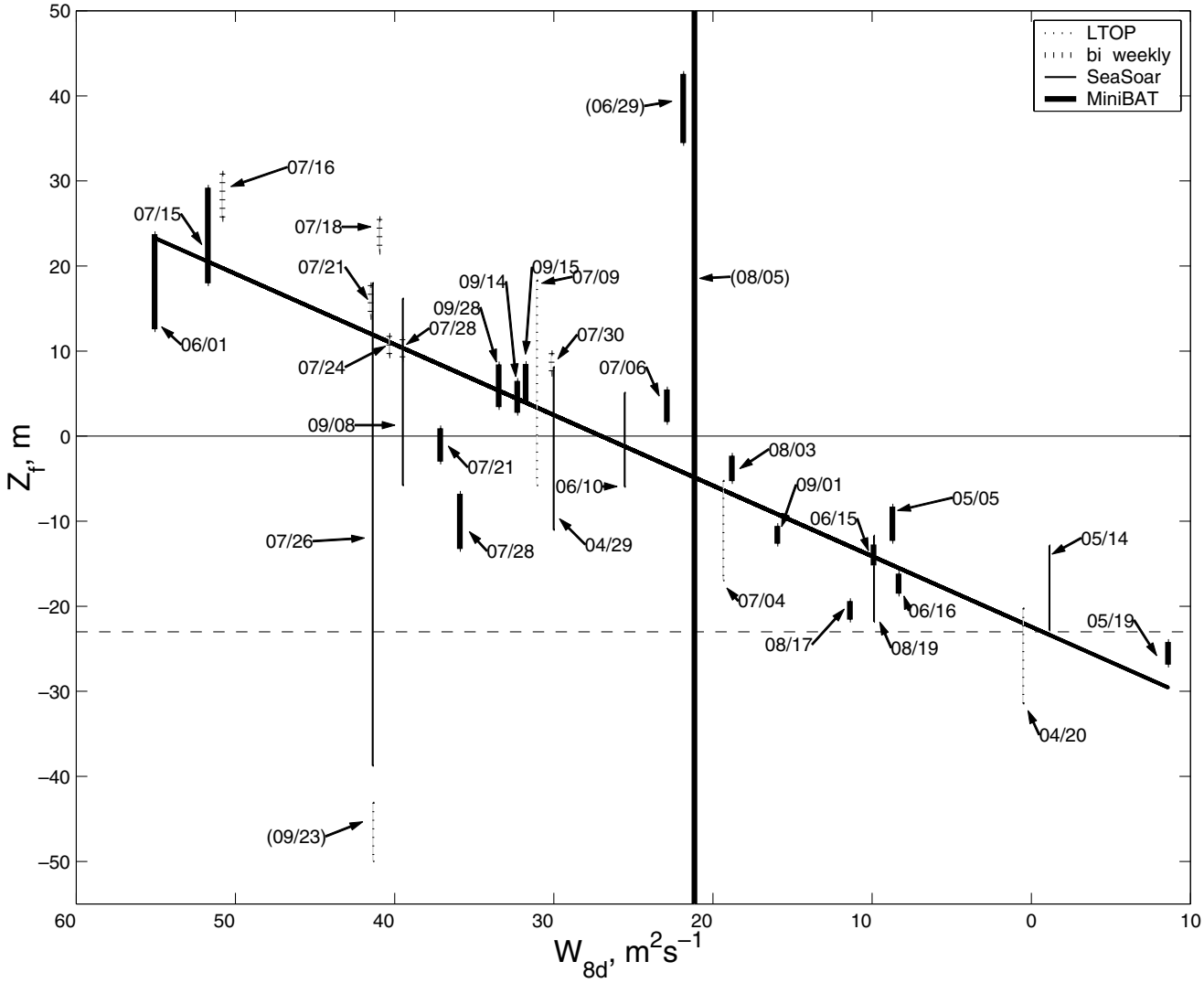

Figure 9. The position of the front as a function of the recent ($k = 8$ days) alongshore wind stress from 33 NH line transects taken during 1999. The error bars represent the uncertainty in the position of the front. Data points not used in the subsequent fits are shown in parentheses. Some of the bars lie on top of each other and are slightly obscured. The dashed line at −23 m represents the "fully relaxed" state estimated by this model.

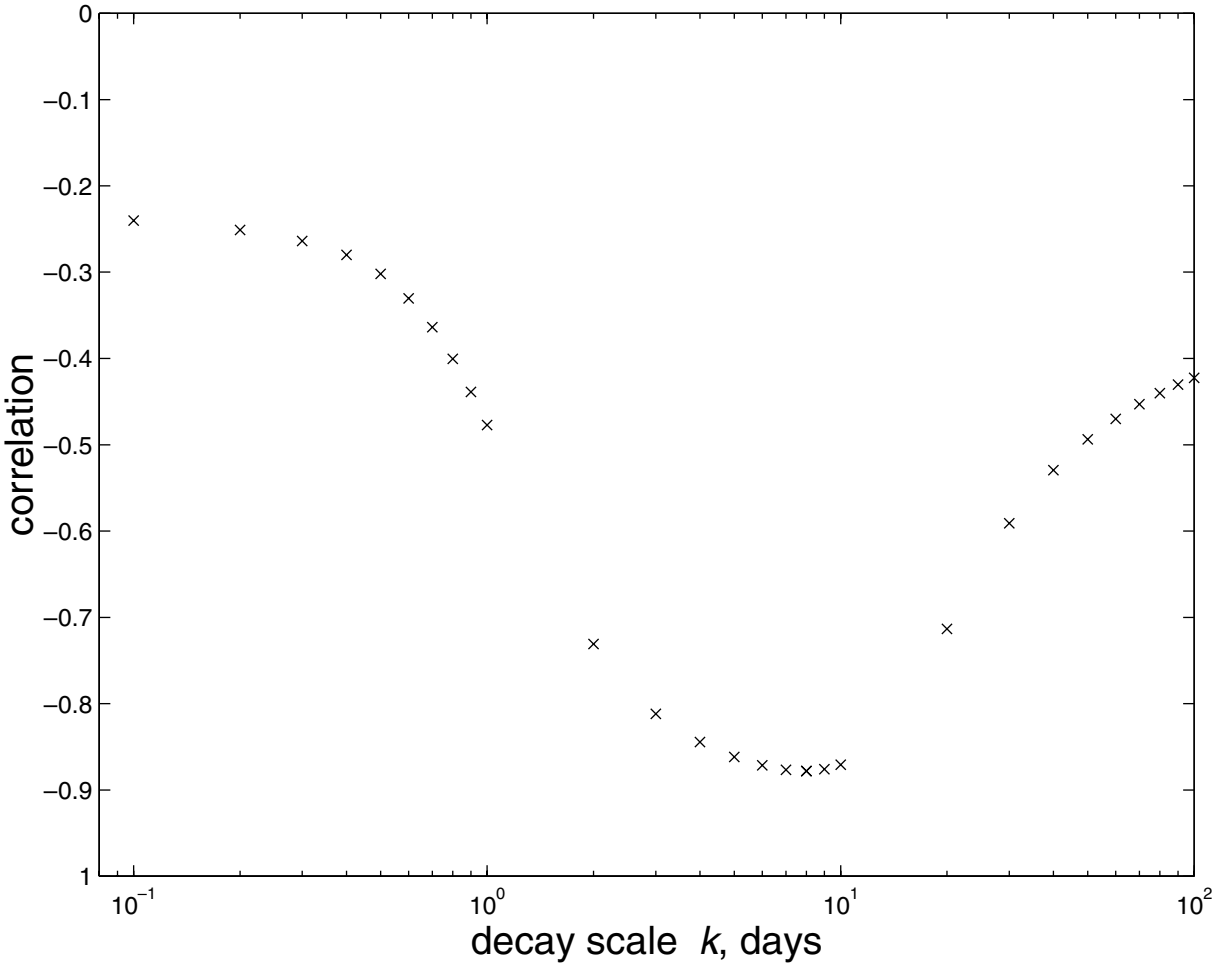

Figure 10. The correlation between the integrated wind stress and the frontal position as a function of the time decay scale k.

isopycnal is on the order of 5 m. Then, normally distributed noise with a variance of 5 m is added to the data repeatedly, and the resulting estimates are used to determine the uncertainty in the estimate of A and R. In this fashion, sections with many, well-distributed data points (such as SeaSoar data), will have relatively small uncertainties, sparse but well distributed data (i.e., GLOBEC-LTOP) or many but poorly distributed points (i.e., MiniBAT, poor in the sense that it covers only a small portion of the shelf) medium errors, and sparse and poorly (for this purpose) distributed data (i.e., NOPP biweekly surveys) the greatest error.

[20] From this, two measures of upwelling intensity, X_f and Z_f, can be calculated:

$$X_f = R \ln\left(\frac{H}{A}\right) \tag{2}$$

and

$$Z_f = -H + A. \tag{3}$$

An example of the fit is shown in Figure 8, for data from the 15 July MiniBAT cruise, where $H = 125$ m, $Z_f = 23$ m, and $R = 51$ km. Although the interpretation of X_f is more intuitive (for $X_f < 0$, it represents the offshore displacement of the outcropped upwelling front), it has the undesirable property of approaching infinity as the front relaxes. For this reason, we will use Z_f for the statistical analysis. Positive values of Z_f represent a fully outcropped pycnocline, and negative values of Z_f represent a more "relaxed" pycnocline. Z_f approaches $-H$ as the front fully relaxes.

[21] These measures of frontal displacement should be proportional to the strength and duration of the alongshore wind stress. Simple two-dimensional theory [*Csanady*, 1977; *Gill*, 1982, p. 404] suggests that indeed the displacement is proportional to the integral of the alongshore wind stress over an indeterminate amount of time. This would suggest that the front off Oregon would become progressively more displaced over the upwelling season, and remain displaced offshore during periods of weak or no alongshore winds. Previous studies have suggested that the alongshore jet is roughly in balance with the upwelling front [*Huyer*, 1977; *Huyer et al.*, 2002]. However, the front tends to relax back toward shore during periods of weak winds, suggesting that the integration should occur over some sort of event timescale. Downwelling favorable winds, which could push the pycnocline back on shore, are too weak and infrequent to account for this relaxation. In order to determine the optimal timescale for an "event" a weighted running mean of the wind stress is used which weights

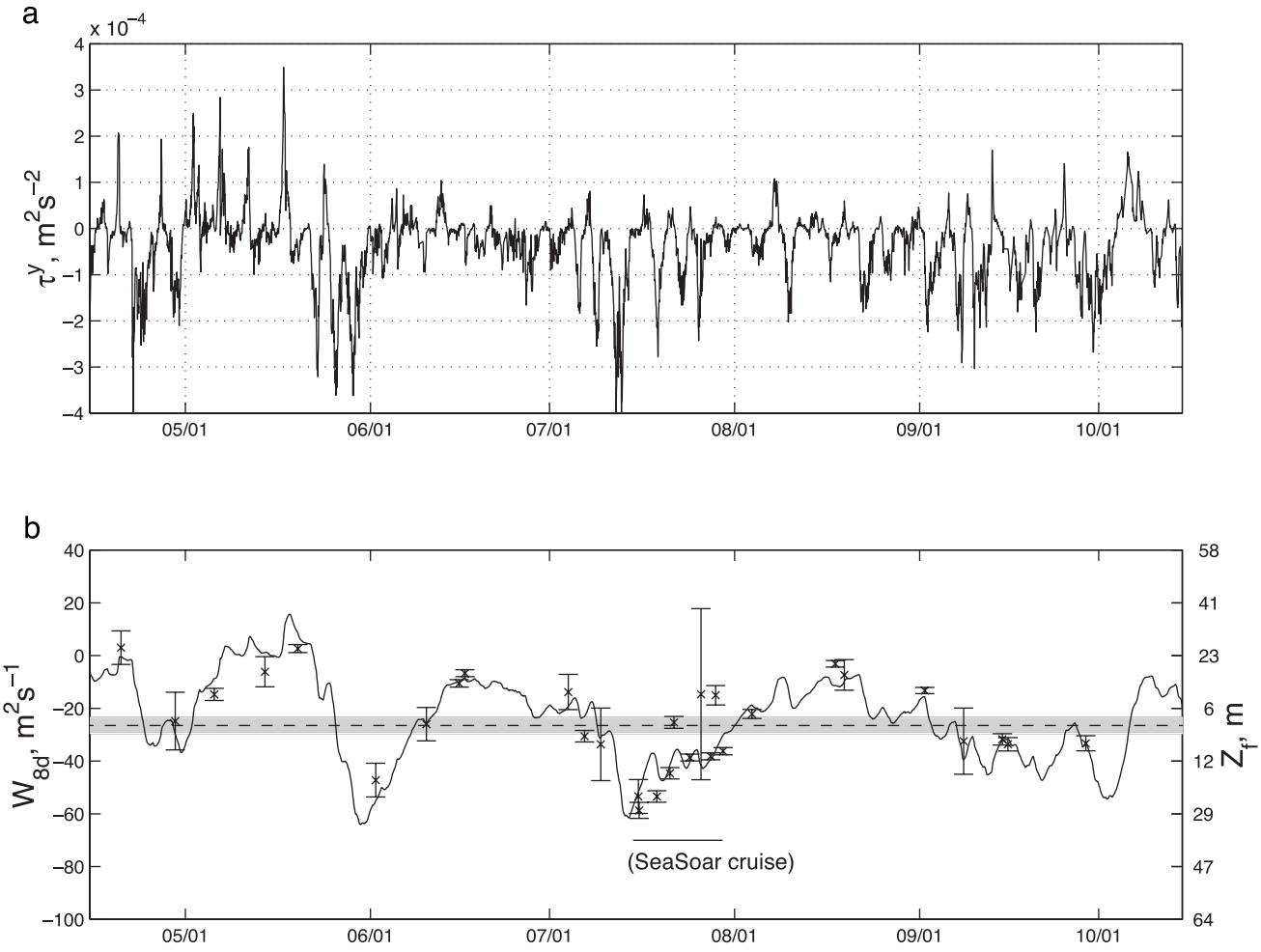

Figure 11. (a) Alongshore wind stress during the 1999 upwelling season taken from NDBC-46050. (b) Alongshore wind stress convoluted with 8 day exponential decay (W_{8d}). The dashed line is the estimated value of W_k sufficient to outcrop the pycnocline ($Z_f > 0$). The gray area is the estimated uncertainty in that estimate. The right-hand axis is the estimated displacement Z_f using the fit values from the hydrographic survey data. The individual data points are the estimated displacements from individual surveys.

the past alongshore wind stress with a decaying exponential. To incorporate a specific timescale, we propose

$$W_k(t) = \int_0^t \frac{\tau^s}{\rho_0} e^{(t'-t)/k} dt' \tag{4}$$

and k is a relaxation timescale to be determined. This is analogous to a damped alongshore jet [*Lentz and Winant*, 1986], and this analogy is discussed in Appendix A.

[22] The position of the front is estimated as a linear function of this wind stress product:

$$Z_f = \alpha W_k + Z_{f0}. \tag{5}$$

The response of the measured upwelling intensity to the wind is determined by α and the relaxed position of the pycnocline by Z_{f0}. The large number of frontal position estimates will allow us to estimate k, α, and Z_{f0} empirically.

4.3. Frontal Position and Wind Stress

[23] Data from several sources were used in this analysis, since the significance of the result increases with the number of frontal position estimates used. These data include four transects as part of the GLOBEC-LTOP, six by the NOPP biweekly survey group, six SeaSoar surveys as part of OSU-NOPP, and 17 MiniBAT cruises as part of OSU-NOPP. Of these 33 cruises, data for three were discarded for the following reasons. On 5 August, the 25.8 σ_t was shallower than 10 m across most of the shelf (MiniBAT survey), the fit was over a very small amount of data and hence the uncertainty of the fit was large. On 23 September (GLOBEC LTOP cruise), the permanent pycnocline shoaled to roughly 40 m depth 140 km offshore, likely due to a large offshore eddy, resulting in a significantly degraded fit and poor estimate of the upwelling intensity. Finally, on 29 June (MiniBAT survey), the upwelling intensity of the hydrographic survey was very strong, but no significant upwelling wind had occurred. It is not known why the 29 June cruise is such a distinct outlier. The moored data [*Boyd et al.*, 2000] show a strong decrease in temperature and increase in salinity around this time as well, which does not appear to be associated with any observed wind event. These three data will be displayed but not used for

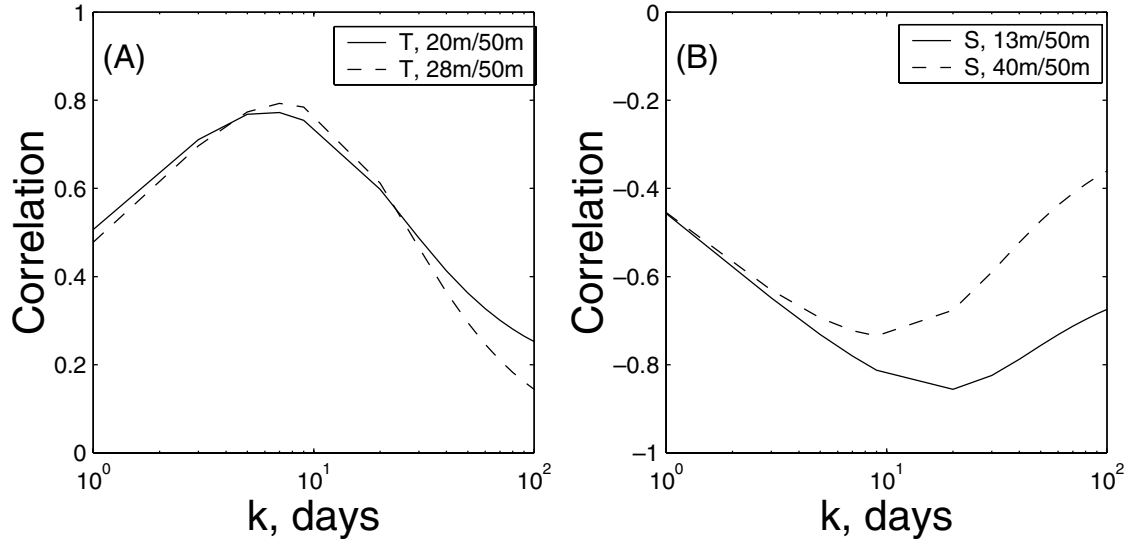

Figure 12. The correlation of low-pass filtered time series of (a) salinity and (b) temperature from the inner-shelf mooring with W_k as a function of k. The correlations are negative for salinity since salinity increases with increasingly negative W_k (strong upwelling). Likewise, the temperature correlations are positive since temperature decreases with increasingly negative W_k.

the subsequent analysis. Table 1 outlines the four programs from which data were used, along with statistics which determine the ''information content'' and hence usefulness of the observational program as it relates to making accurate estimates of the frontal position. These data will be used for the analysis of the relationship between the frontal position and the wind stress.

[24] The result of this analysis (Figure 9) suggests a strong relationship between the upwelling position and the weighted running mean alongshore wind stress. With a decay constant of approximately $k = 8$ days, the absolute values of the correlation is approximately 0.88. This is highly significant for 30 independent measurements (this calculation was performed disregarding data from the 29 June, 5 August, and 23 September surveys). The decay constant was chosen empirically, by computing the correlation between the wind stress product and the frontal positions for a large range of potential decay timescales (Figure 10). The correlation is strong for a wide range of timescales, with absolute values of correlations greater than 0.85 for a range of roughly 5–12 days. This timescale is roughly consistent with moored data from the same season (see Discussion). The correlation as a function of k shows that the correlation is poor both for small k (equivalent to equating upwelling intensity to the wind measured at the time of the survey) and with large k (equivalent to integrating over the entire upwelling season).

[25] Given the optimal timescale k, the frontal data (Z_f) are fit to the weighted wind data (W_k) using a weighted least squares technique (data being weighted in inverse proportion to its uncertainty). This relationship can be used as a ''rule of thumb'' for determining the status of the pycnocline given recent wind conditions. In this case, it appears that the pycnocline is fully upwelled ($Z_f > 0$) for values of the integrated wind stress W_k less than roughly -28 ± 3 m^2 s^{-1}. This quantifies the sufficiently strong steady wind required to outcrop the main pycnocline. Figure 11 shows the time series of the wind stress and the running weighted mean wind stress for the 1999 season. From the weighted running mean, we would expect the main pycnocline to be outcropped form middle to late July (coincidentally, when the R/V *Wecoma* was making the OSU-NOPP SeaSoar surveys [*Barth et al.*, 2001]) and remained outcropped through much of September under the influence of weaker but steadier winds.

[26] Six MiniBAT surveys were made during the 2000 upwelling season (Austin, unpublished data). Of these, five fall on the ''best fit'' line estimated with the 1999 data. The sixth is an outlier not unlike the 29 June 1999 survey. These data were not used in the calculation of the fit shown here. It would be a worthwhile exercise to do the same computations for other years in which large amounts of high-resolution hydrographic data were collected, in order to determine whether the constants estimated here regarding the relationship between the wind stress and the frontal position are representative of just 1999, or are constant over time.

[27] The linear fit has an intercept at approximately $Z_{f0} = -23$ m, suggesting that the pycnocline relaxes to a state where an extrapolated 25.8 σ_t isopycnal would intersect the ''coastal wall'' ($x = 0$) about 23 m below the surface. This suggests that the relaxed state is dynamic, in geostrophic balance with an alongshore jet. This is consistent with the basic paradigm that there is mean equatorward current during the upwelling season, even in the absence of alongshore wind stress [*Huyer et al.*, 2002].

5. Discussion

5.1. Moored Data

[28] Hydrographic data were collected at a set of moorings [*Boyd et al.*, 2000] placed on the 50, 80, and 130 m

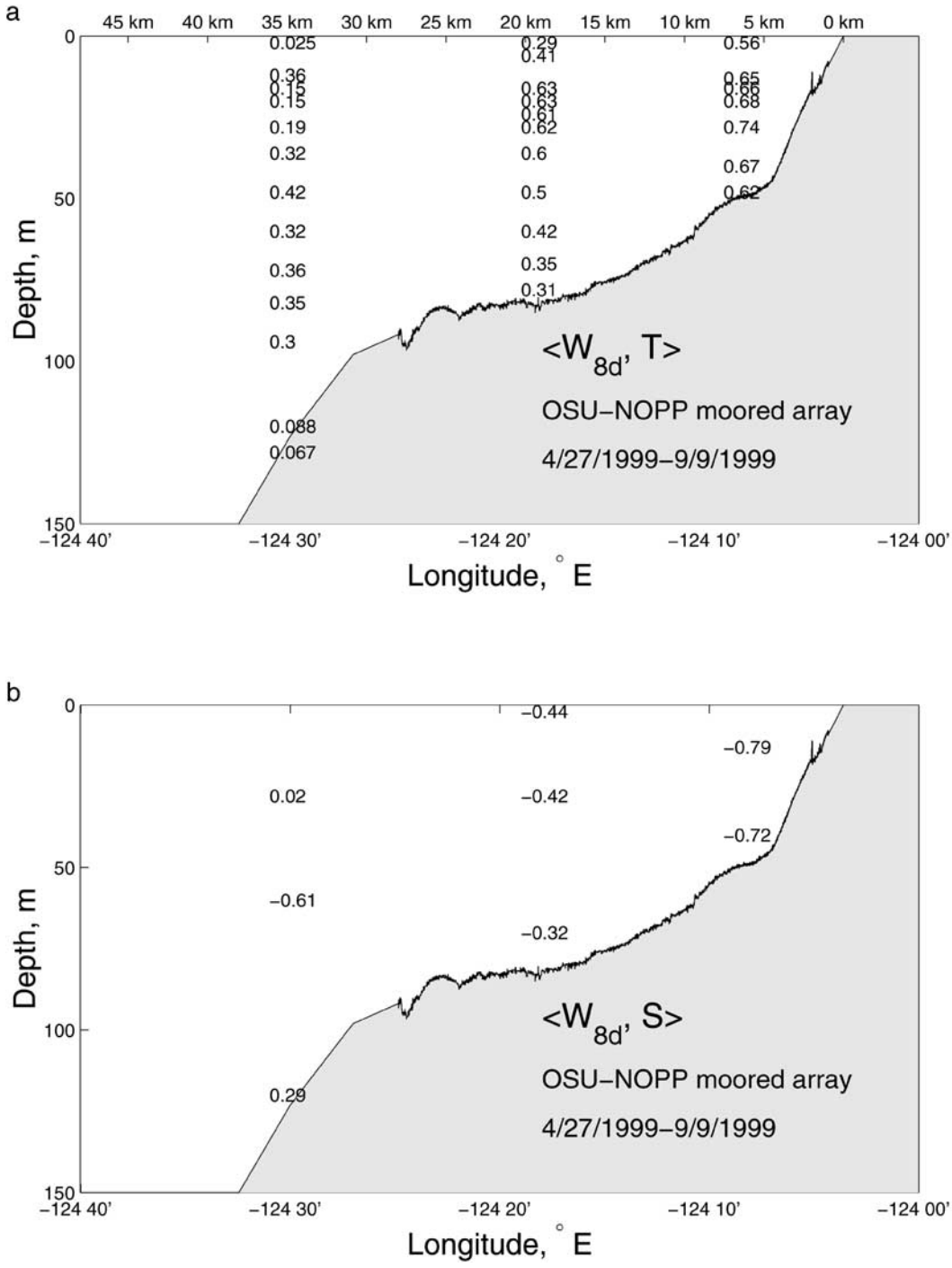

Figure 13. The correlation of low-pass filtered (a) temperature and (b) salinity time series from all three moorings with W_{8d}.

isobaths between April and September 1999. The timescale of relaxation is evident in this moored hydrographic data as well as the CTD surveys. An analysis similar to that of the previous section applied to low-passed hydrographic time series from several hydrographic mooring elements suggests very similar timescales for k. A process analogous to that used to produce Figure 10, which was used to estimate the optimal timescale k, was applied to four moored hydrographic elements (salinity at 13 and 40 m on the 50 m isobath, and temperature at 20 and 28 m on the 50 m isobath). Each of these displayed an optimum timescale of relaxation between 7 and 20 days (Figure 12), roughly consistent with the previous analysis. The correlation between the alongshore wind stress product and the salinity is negative since the more negative W_k becomes (more strongly upwelling favorable) the greater the salinity

becomes. Conversely, the temperature decreases, resulting in positive correlations.

[29] Correlations between W_{8d} (shorthand for the quantity defined in equation (4), calculated with k = 8 days, the optimum weighting timescale for the CTD sections) and all of the moored elements (Figure 13) show high correlations (roughly 0.7) at the inner shelf and weaker correlations offshore, where the upwelling plays a smaller role in hydrographic variation.

5.2. Relaxation

[30] There are several methods that may be responsible for the relaxation response observed after an upwelling event. It is possible that baroclinic instability in the upwelling jet [i.e., *Barth*, 1994] may redistribute momentum over the shelf leading to relaxation. *Send et al.* [1987] attribute part of the relaxation response observed during the CODE experiment to surface heating. However, in this case, we see relaxation of the salinity field as well, for which such a process could not be responsible. *Send et al.* [1987] also discuss the role of alongshore pressure gradients created during upwelling events. Alongshore variation in upwelling conditions may lead to alongshore transport divergence and hence regions of high or low pressure, and the opposing pressure gradients drive alongshore flow. This alongshore flow, in turn, drives transport in the bottom Ekman layer counter to that in the bottom Ekman layer during the wind event. These reversals appear in the alongshore current field almost simultaneously along the coast during wind relaxations (B. Grantham, Oregon State University, unpublished data), suggesting that it is a regional and not a local response. This behavior is explored in a model of the CODE region off of California by *Gan and Allen* [2002]. The missing piece of this puzzle is developing an understanding of what alongshore features give rise to these pressure gradients, and how the timescale of relaxation are related to scales of alongshore variation.

5.3. Summary

[31] Hydrographic data from a series of small towed-vehicle cruises have been combined with similar hydrographic data collected during the 1999 field season on the Oregon shelf to show a strong relationship between upwelling intensity and the alongshore wind stress. This relationship suggests that the pycnocline relaxes back toward a rest state after an upwelling-favorable wind event on an e-folding timescale of roughly 8 days. The relationship between the upwelling intensity and the alongshore wind stress can be used to estimate the duration of the outcropping of the main pycnocline, which plays a major role in driving the coastal food chain by bringing nutrient-rich water into the euphotic zone.

6. Appendix A

[32] A simple model of the vertically averaged alongshore momentum balance includes surface and bottom stress and an acceleration term [*Lentz and Winant*, 1986]:

$$\frac{dV}{dt} = \frac{\tau^s}{h\rho_0} - \frac{r}{h}V, \tag{6}$$

where V is the vertically averaged alongshore velocity, τ^s the alongshore wind stress, r a frictional parameter, and h the local water depth. The solution of (6) is

$$V(t) = \int_0^t \frac{\tau^s}{\rho_0} e^{\frac{r}{h}(t-t')} dt' + V(0)e^{-\frac{r}{h}t}. \tag{7}$$

This solution suggests that given some sort of relaxation mechanism (in this case, parameterized as bottom friction), the alongshore velocity should decay on some timescale inversely proportional to the friction. It should be noted that this specific formulation is technically incorrect in this particular instance because the alongshore velocity in an upwelling jet is by definition baroclinic, in thermal wind balance with the upwelling front. Therefore, the vertical average alongshore velocity does not reflect the bottom velocity. Bottom friction is only used as an analogy.

[33] Setting $\frac{h}{r}$ = 8d, with a linear coefficient of friction of 5×10^{-4} m s^{-1} [*Lentz and Winant*, 1986], yields $h \approx 350$ m, far deeper than the water, as the relaxation is observed in mooring data to occur almost simultaneously across the entire shelf. This suggests, unsurprisingly, that the relaxation is not simply a matter of dissipation of alongshore momentum by bottom friction. Similarly, the optimum timescale of relaxation appears constant across the shelf, using moored temperature records from several different locations.

[34] **Acknowledgments.** Thanks go to Mike Kosro, who helped with the initial acquisition of the MiniBAT system, and to Steve Pierce and Walt Waldorf, who helped with the 1999 MiniBAT field season, both in the lab and on board. Ron Barrell was the captain of the R/V *Sacajawea* for all of the cruises and was a tremendous help, and Fred Jones provided dockside support. Tim Boyd, Murray Levine, and Mike Kosro kindly provided moored data from OSU-NOPP. Jane Huyer and Bob Smith provided the LTOP data used in the paper. Bill Peterson and Leah Feinberg provided CTD data from their 1999 NOPP sampling cruises. Pat Wheeler and Holly Corwith provided the nutrient data. Conversations and suggestions from Peter Oke and Jonathan Nash helped in the analysis portion of this paper. Two anonymous reviewers provided insightful comments that improved the manuscript. This research was supported by the National Oceanographic Partnership Program, Office of Naval Research grant N00014-98-1-0787.

References

Austin, J. A., J. A. Barth, and S. D. Pierce, Small-boat hydrographic surveys of the Oregon mid- to inner shelf, May–September 1999, Data Rep. 178, Ref. 00-2, Coll. of Oceanic and Atmos. Sci., Oreg. State Univ., Corvallis, Oreg., April 2000.

Barth, J. A., Short wavelength instabilities on coastal jets and fronts, *J. Geophys. Res.*, *99*, 16,095, 1994.

Barth, J. A., R. O'Malley, A. Y. Erofeev, J. Fleischbein, S. D. Pierce, and P. M. Kosro, SeaSoar CTD observations from the central Oregon shelf, W9907C, 13–31 July 1999, Data Rep. 184, Ref. 2001-5, Coll. of Oceanic and Atmos. Sci., Oreg. State Univ., Corvallis, Oreg., 2001.

Boyd, T., M. D. Levine, P. M. Kosro, and S. R. Gard, Mooring observations from the Oregon continental shelf, April–September 1999, Data Rep. 177, Ref. 00-1, Coll. of Oceanic and Atmos. Sci., Oreg. State Univ., Corvallis, Oreg., April 2000.

Collins, C. A., C. N. K. Mooers, M. R. Stevenson, R. L. Smith, and J. G. Patullo, Direct current measurements in the frontal zone of a coastal upwelling region, *J. Oceanogr. Soc. Jpn.*, *24*, 295, 1968.

Csanady, G. T., Intermittent "full" upwelling in Lake Ontario, *J. Geophys. Res.*, *82*, 397, 1977.

Ekman, V. W., On the influence of the Earth's rotation on ocean-currents, *Arch. Math. Astron. Fys.*, *2*, 1–53, 1905.

Fairall, C. W., E. F. Bradley, D. P. Rogers, J. B. Edson, and G. S. Young, Bulk parameterization of air–sea fluxes for Tropical Ocean-Global Atmospheric Coupled-Ocean Atmospheric Response Experiment, *J. Geophys. Res.*, *101*, 3747–3764, 1996.

Fleischbein, J., A. Huyer, R. L. Smith, H. Corwith, W. Moses, and P. A.

Wheeler, Hydrographic data from the GLOBEC Long-Term Observation Program off Oregon, 1999 and 2000, 298 pp., Data Rep. 183, Ref. 01-3, Coll. of Oceanic and Atmos. Sci., Oreg. State Univ., Corvallis, Oreg., 2001.

Gan J., and J. S. Allen, A modeling study of shelf circulation off northern California in the region of the Coastal Ocean Dynamics Experiment: Response to relaxation of upwelling winds, *J. Geophys. Res.*, *107*(C9), 3123, doi:10.1029/2000JC000768, 2002.

Gill, A. E., *Atmosphere–Ocean Dynamics*, 666 pp., Academic, San Diego, Calif., 1982.

Halpern, D., Variations in the density field during coastal upwelling, *Tethys*, *6*, 363, 1974.

Halpern, D., Structure of a coastal upwelling event observed off Oregon during July 1973, *Deep Sea Res.*, *23*, 495, 1976.

Huyer, A., Seasonal variation in temperature, salinity, and density over the continental shelf off Oregon, *Limnol. Oceanogr.*, *22*, 442–453, 1977.

Huyer, A., Hydrographic observations along the CODE Central Line off Northern California, 1981, *J. Phys. Oceanogr.*, *14*, 1647, 1984.

Huyer, A., and R. L. Smith, A subsurface ribbon of cool water over the continental shelf of Oregon, *J. Phys. Oceanogr.*, *4*, 381, 1974.

Huyer, A., R. D. Pillsbury, and R. L. Smith, Seasonal variation of the alongshore velocity field over the continental shelf off Oregon, *Limnol. Oceanogr.*, *20*, 90, 1975.

Huyer A., R. L. Smith, and J. Fleischbein, The coastal ocean off Oregon and northern California during the 1997–1998 El Niño, *Prog. Oceanogr.*, *54*, 311–341, 2002.

Kelly, K. A., Swirls and plumes or application of statistical methods to satellite-derived sea-surface temperatures, Ph.D. thesis, 210 pp., Scripps Inst. of Oceanogr., La Jolla, Calif., 1983.

Lentz, S. J., The surface boundary layer in coastal upwelling regions, *J. Phys. Oceanogr.*, *22*, 1517, 1992.

Lentz, S. J., and C. D. Winant, Subinertial currents on the southern California shelf, *J. Phys. Oceanogr.*, *16*, 1737, 1986.

Mooers, C. N. K., C. A. Collins, and R. L. Smith, The dynamic structure of the frontal zone in the coastal upwelling region off Oregon, *J. Phys. Oceanogr.*, *6*, 3, 1976.

Pak, H., G. F. Beardsley, and R. L. Smith, An optical and hydrographic study of a temperature inversion off Oregon during upwelling, *J. Geophys. Res.*, *75*, 629, 1970.

Pollard, R. T., Frontal surveys with a towed profiling conductivity/temperature/depth measurement package (SeaSoar), *Nature*, *22*, 433, 1986.

Send, U., R. C. Beardsley, and C. D. Winant, Relaxation from upwelling in the Coastal Ocean Dynamics Experiment, *J. Geophys. Res.*, *92*, 1683, 1987.

Small, L. F., and D. W. Menzies, Patterns of primary productivity and biomass in a coastal upwelling region, *Deep Sea Res.*, *28A*, 123, 1981.

Winant, C. D., R. C. Beardsley, and R. E. Davis, Moored wind, temperature, and current observations made during Coastal Ocean Dynamics Experiments 1 and 2 over the northern California continental shelf and upper slope, *J. Geophys. Res.*, *92*, 1569, 1987.

J. A. Austin, Center for Coastal Physical Oceanography, Old Dominion University, Norfolk, VA 23507, USA. (jay@ccpo.odu.edu)

J. A. Barth, College of Oceanic and Atmospheric Sciences, Oregon State University, 104 Ocean Administration, Corvallis, OR 97331, USA.